

Reactions of *cis* and *trans* Bcat, Aryl Osmium Complexes (cat = 1,2-O₂C₆H₄). Bis(Bcat) Complexes of Osmium and Ruthenium and a Structural Comparison of *cis* and *trans* Isomers of Os(Bcat)I(CO)₂(PPh₃)₂

Clifton E. F. Rickard, Warren R. Roper,^{*,†} Alex Williamson, and L. James Wright*

Department of Chemistry, The University of Auckland, Private Bag 92019, Auckland, New Zealand

Received May 31, 2000

Reaction of Os(Bcat)Cl(CO)(PPh₃)₂ (**1**) (HBcat = catecholborane or 1,3,2-benzodioxaborole) with *o*-tolyllithium gives the yellow, five-coordinate Bcat, aryl complex Os(Bcat)(*o*-tolyl)(CO)(PPh₃)₂ (**2**). Treatment of **2** with carbon monoxide or *p*-tolylisocyanide gives the corresponding saturated Bcat, aryl complexes *cis*-Os(Bcat)(*o*-tolyl)(CO)₂(PPh₃)₂ (**3**) and *cis*-Os(Bcat)(*o*-tolyl)(CO)(CN-*p*-tolyl)(PPh₃)₂ (**4**). Complexes **3** and **4** decompose in benzene solution at room temperature to give *o*-tolylBcat and the orthometalated triphenylphosphine complexes Os(C₆H₄PPh₂)H(CO)₂(PPh₃) (**5**) and Os(C₆H₄PPh₂)H(CO)(CN-*p*-tolyl)(PPh₃) (as a mixture of two isomers, **6a** and **6b**), respectively. In the presence of B₂cat₂, **3** and **4** react to give the bis(Bcat) complexes Os(Bcat)₂(CO)₂(PPh₃)₂ (**7**) and Os(Bcat)₂(CO)(CN-*p*-tolyl)(PPh₃)₂ (**8**). Complex **3** also reacts with HBcat to produce Os(Bcat)H(CO)₂(PPh₃)₂ (**9**). The bis(Bcat) ruthenium complexes Ru(Bcat)₂(CO)₂(PPh₃)₂ (**10**) and Ru(Bcat)₂(CO)(CN-*p*-tolyl)(PPh₃)₂ (**11**) can be prepared by treatment of Ru(CO)₂(PPh₃)₃ or Ru(CO)(CN-*p*-tolyl)(PPh₃)₃ with B₂cat₂. Complex **3** reacts with Cl₂C=CCl₂ or CHCl₃ to produce OsCl(CCl=CCl₂)(CO)₂(PPh₃)₂ (**12**) or OsCl₂(CO)₂(PPh₃)₂, respectively. Complex **1** when treated with CO gives *cis*-Os(Bcat)Cl(CO)₂(PPh₃)₂ (**13**), which in turn with phenyllithium or *o*-tolyllithium gives *trans*-Os(Bcat)(Ph)(CO)₂(PPh₃)₂ (**14**) or *trans*-Os(Bcat)(*o*-tolyl)(CO)₂(PPh₃)₂ (**15**). Complex **15** reacts with I₂ to give a mixture of *trans*-Os(Bcat)I(CO)₂(PPh₃)₂ (**16**) and *trans*-Os(*o*-tolyl)I(CO)₂(PPh₃)₂ (**17**). Complex **16** is also formed by heating *cis*-Os(Bcat)I(CO)₂(PPh₃)₂ (**18**) in benzene. Crystal structures of complexes, **5**, **8**, **10**, **11**, **12**, **16**, and **18** are reported.

Introduction

Compounds with transition metal–boron, 2c-2e bonds (L_{*n*}M–BR₂) have been widely studied in the past decade primarily because of the recognition that these compounds are key intermediates in the metal-catalyzed syntheses of boron-functionalized organics. Several reviews have covered developments in this area.^{1–3} In this paper we examine two features central to the role of metal boryl complexes as catalysts in organic transformations. The first of these involves the synthesis of metal complexes containing *both* boryl and σ -bound carbon ligands, L_{*n*}M(BR₂)R, and studies of the reductive elimination of BR₃ from these complexes. The second involves the collection of further information on the nature of the metal–boron bond, through a structural

comparison of *cis*- and *trans*-isomers of Os(Bcat)I(CO)₂(PPh₃)₂. Some preliminary results from this work, specifically the preparation and characterization of the five-coordinate *o*-tolyl, Bcat complex, Os(Bcat)(*o*-tolyl)(CO)(PPh₃)₂ (**2**), have already been published as a Communication.⁴

Results and Discussion

Reductive Elimination of *o*-Tolyl-Bcat from *cis*-*o*-Tolyl, Bcat Complexes in the Absence of Other Reactants. Reaction between the previously reported coordinatively unsaturated osmium boryl complex Os(Bcat)Cl(CO)(PPh₃)₂ (**1**)⁵ and *o*-tolyllithium produces the five-coordinate boryl, aryl complex Os(Bcat)(*o*-tolyl)(CO)(PPh₃)₂ (**2**).⁴ Treatment of **2** with either carbon monoxide or *p*-tolylisocyanide produces the corresponding saturated complexes *cis*-Os(Bcat)(*o*-tolyl)(CO)₂(PPh₃)₂ (**3**)⁴ and *cis*-Os(Bcat)(*o*-tolyl)(CO)(CN-*p*-tolyl)(PPh₃)₂ (**4**), respectively (see Scheme 1). The spectroscopic

* Corresponding author. Phone: +64 9 373 7599 ext 8320. Fax: +64 9 373 7422.

[†] E-mail: w.roper@auckland.ac.nz.

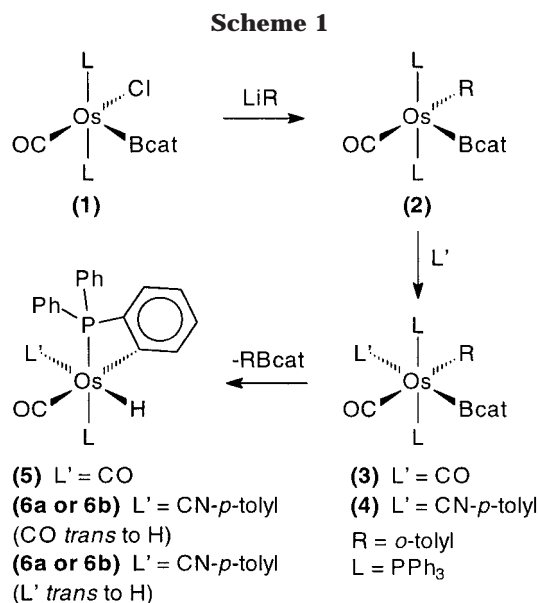
(1) Wadepohl, H. *Angew. Chem., Int. Ed. Engl.* **1997**, *36*, 2441.

(2) Braunschweig, H. *Angew. Chem., Int. Ed. Engl.* **1998**, *37*, 1786.

(3) (a) Irvine, G. J.; Lesley, M. J. G.; Marder, T. B.; Norman, N. C.; Rice, C. R.; Robins, E. G.; Roper, W. R.; Whittell, G. R.; Wright, L. J. *Chem. Rev.* **1998**, *98*, 2685. (b) Marder, T. B.; Norman, N. C. *Topics in Catalysis*; Leitner, W., Blackmond, D. G., Ed.; Baltzer Science Publishers: Amsterdam, 1998; Vol. 5, p 63. (c) Smith, M. R., III. *Prog. Inorg. Chem.* **1999**, *48*, 505. (d) Chen, H.; Hartwig, J. F. *Angew. Chem., Int. Ed. Engl.* **1999**, *38*, 3391.

(4) Rickard, C. E. F.; Roper, W. R.; Williamson, A.; Wright, L. J. *Angew. Chem., Int. Ed.* **1999**, *38*, 1110.

(5) (a) Irvine, G. J.; Roper, W. R.; Wright, L. J. *Organometallics* **1997**, *16* (6), 2291. (b) Rickard, C. E. F.; Roper, W. R.; Williamson, A.; Wright, L. J. *Organometallics* **1998**, *17*, 4869.



data for **4**, and for all other new compounds reported in this paper, are presented in Table 1 (IR), Table 2 (¹H NMR), Table 3 (¹³C NMR), and Table 4 (¹¹B NMR). The ¹¹B NMR data are not particularly informative because there is only a very small variation in the ¹¹B chemical shifts over all the compounds measured. Apart from the following two generalizations, these data will not be further discussed in this paper. First, the one five-coordinate compound measured, Os(Bcat)(*o*-tolyl)(CO)(PPh₃)₂ (**2**), has a ¹¹B chemical shift value significantly further upfield than the values for the six-coordinate Bcat complexes. Second, where comparison can be made between corresponding ruthenium and osmium complexes, the ruthenium complexes show chemical shifts at lower field values.

Complex **3** slowly decomposes in benzene solution at room temperature to give *o*-tolyl-Bcat and the orthometalated complex Os(C₆H₄PPh₂)H(CO)₂(PPh₃) (**5**).⁶ The nature of **5** was confirmed both by comparing the IR spectrum with that of an authentic sample⁶ and by an X-ray crystal structure determination, which is reported in this paper. The first step in the formation of **5** is most likely the reductive elimination of *o*-tolyl-Bcat, giving the reactive, four-coordinate species "Os(CO)₂(PPh₃)₂", which, in the absence of a suitable reactant, undergoes orthometalation to form Os(C₆H₄PPh₂)H(CO)₂(PPh₃) (see Scheme 1). The reductive elimination of *o*-tolyl-Bcat in CDCl₃ was monitored by ¹H NMR spectroscopy and found to be approximately half completed, at 25 °C, after 100 min. Under these conditions the osmium complex formed is OsCl₂(CO)₂(PPh₃)₂, which results from reaction of "Os(CO)₂(PPh₃)₂" with the solvent (see below).

Complex **4** also readily eliminates *o*-tolyl-Bcat to give the orthometalated complex Os(C₆H₄PPh₂)H(CO)(CN-*p*-tolyl)(PPh₃) (**6**), as a mixture of two isomers (**6a** and **6b**). These have not been separated, but both have the two phosphorus atoms arranged mutually *trans*, as shown by the large *J*_{PP} values observed in the ³¹P NMR spectrum (see Experimental Section). In the ¹H NMR

spectrum the hydride signals for each isomer appear as a doublet of doublets, and these multiplicities, together with the chemical shift positions, are indicative of the geometries with *trans* phosphorus atoms, as indicated in Scheme 1. No absolute assignment of the two isomers (**6a** or **6b**) has been made. The facile B–C bond formation observed in the chemistry discussed above, resulting from reductive elimination of *cis* boryl and σ -bound carbon ligands, is a step that has been postulated to occur both in metal-catalyzed hydroborations^{1,2} and in the borylation of arenes as described by Hartwig.⁷ It should be noted also that theoretical studies have predicted very low barriers to reductive eliminations of this type.^{8,9}

Reductive Elimination of *o*-Tolyl-Bcat from *cis*-*o*-Tolyl, Bcat Complexes in the Presence of Compounds with B–H and B–B Bonds. An important mechanistic step often proposed in metal-catalyzed hydroborylation or diborylation of alkenes/alkynes is the oxidative addition of a B–H bond or B–B bond to a reactive intermediate, thus regenerating complexes with M–B bonds and so maintaining the catalytic cycle. Reductive elimination of *o*-tolyl-Bcat from complexes **3** or **4** (giving the four-coordinate complexes "Os(CO)₂(PPh₃)₂" and "Os(CO)(CN-*p*-tolyl)(PPh₃)₂" in the presence of B₂cat₂ produces the bis(boryl) complexes Os(Bcat)₂(CO)₂(PPh₃)₂ (**7**) and Os(Bcat)₂(CO)(CN-*p*-tolyl)(PPh₃)₂ (**8**), respectively (Scheme 2), thereby modeling two consecutive steps for the proposed catalyzed addition of a B–B bond in diborylation reactions. Complexes **7** and **8** are the first reported bis(boryl) complexes of osmium, and both contain *cis*-disposed phosphine ligands, *cis*-Bcat ligands, and *trans*-carbonyl ligands. The structure of complex **8** was confirmed by X-ray crystallography (see below).

The corresponding ruthenium bis(boryl) complexes Ru(Bcat)₂(CO)₂(PPh₃)₂ (**10**) and Ru(Bcat)₂(CO)(CN-*p*-tolyl)(PPh₃)₂ (**11**) can be prepared by a direct oxidative addition of B₂cat₂ to the zero oxidation state complexes Ru(CO)₂(PPh₃)₃ or Ru(CO)(CN-*p*-tolyl)(PPh₃)₃ (Scheme 3). Complexes **10** and **11** were both characterized by X-ray crystallography (see below), and the arrangements of the ligands are similar to that of the osmium complex **8**. It should be noted that the osmium bis(Bcat) complexes **7** and **8** are not accessible through oxidative addition of B₂cat₂ to the corresponding osmium zero oxidation state complexes.

Reductive elimination of *o*-tolyl-Bcat from complex **3** in the presence of HBcat cleanly produces Os(Bcat)H(CO)₂(PPh₃)₂ (**9**) (Scheme 2), thereby modeling both the key product-forming step and the catalyst-regenerating step in catalytic hydroboration reactions. The triphenylphosphine ligands in **9** are mutually *trans*, as indicated by both the ¹H and ¹³C NMR spectra, and the presence of two carbonyl bands in the IR spectrum indicates that the two carbonyl ligands are mutually *cis*.

The above observations make it clear that complex **3** can serve as a convenient precursor for "Os(CO)₂(PPh₃)₂" and treatment of **3** with Cl₂C=CCl₂ or CHCl₃ gives

(7) Waltz, K. M.; Muhoro, C. N.; Hartwig, J. F. *Organometallics* **1999**, *18*, 3383.

(8) (a) Musaeve, D. G.; Mebel, A. M.; Morokuma, K. *J. Am. Chem. Soc.* **1994**, *116*, 10693. (b) Dorigo, A. E.; von R. Schleyer, P. *Angew. Chem., Int. Ed. Engl.* **1995**, *34*, 115.

(9) Sakaki, S.; Kai, S.; Sugimoto, M. *Organometallics* **1999**, *18*, 4825.

(6) Clark, G. R.; Headford, C. E. L.; Marsden, K.; Roper, W. R. *J. Organomet. Chem.* **1982**, *231*, 335.

Table 1. Infrared Data (cm⁻¹)^a for Ruthenium and Osmium Boryl Complexes and Derived Complexes

complex	$\nu(\text{C}=\text{O})$	$\nu(\text{C}=\text{N})$	other bands ^b
<i>cis</i> -Os(Bcat)(<i>o</i> -tolyl)(CO)(CN- <i>p</i> -tolyl)(PPh ₃) ₂ (4)	1941s	2097s	1237m, 1117m, 1081s, 1005w, 813m 1884m ^c
$\text{Os}(\text{C}_6\text{H}_4\text{PPh}_2)\text{H}(\text{CO})_2(\text{PPh}_3)$ (5)	2009vs, 1956vs		
$\text{Os}(\text{C}_6\text{H}_4\text{PPh}_2)\text{H}(\text{CO})(\text{CN-}i\text{-tolyl})(\text{PPh}_3)$ (6)	1959m, br, 1935m, br, 1913m, br ^e	2089m,br	
Os(Bcat) ₂ (CO)(CN- <i>p</i> -tolyl)(PPh ₃) ₂ (8)	1964vs	2141m	1236s, 1128m, 1102s, 1072s, 1011m, 811w 1895s, ^c 1235s, 1135m, 1015m, 813w
Os(Bcat)H(CO) ₂ (PPh ₃) ₂ (9)	1971s, 2009s		1236s, 1137m, 1112s, 1104m, 1072s, 1027w, 811w
Ru(Bcat) ₂ (CO) ₂ (PPh ₃) ₂ (10)	1975vs, 2057w		1235s, 1119m, 1063s, 1012m, 809m
Ru(Bcat) ₂ (CO)(CN- <i>p</i> -tolyl)(PPh ₃) ₂ (11)	1974vs	2141s	
Os(CCl=CCl ₂)Cl(CO) ₂ (PPh ₃) ₂ (12)	2027vs, 1952vs		
<i>cis</i> -Os(Bcat)Cl(CO) ₂ (PPh ₃) ₂ (13)	2025m, 1965m, 1941vs ^d		1231m, 1149w, 1109m, 1031w, 813w
<i>trans</i> -Os(Bcat)(Ph)(CO) ₂ (PPh ₃) ₂ (14)	1948vs, 1920w		1234m, 1121m, 1083s, 1104m, 809w
<i>trans</i> -Os(Bcat)I(CO) ₂ (PPh ₃) ₂ (16)	1970vs, 2064w		1235m, 1135w, 1092s, 1028w, 810w
<i>cis</i> -Os(Bcat)I(CO) ₂ (PPh ₃) ₂ (18)	2020s, 1958vs		1237s, 1149m, 1116s, 1099s, 1029m, 814w

^a Spectra recorded as Nujol mulls between KBr plates. ^b Bands associated with boryl ligand unless denoted otherwise. ^c $\nu(\text{OsH})$. ^d Solid-state splitting. ^e Distinction between $\nu(\text{CO})$ and $\nu(\text{OsH})$ has not been made.

OsCl(CCl=CCl₂)(CO)₂(PPh₃)₂ (**12**) and OsCl₂(CO)₂(PPh₃)₂, respectively (Scheme 4). An X-ray crystallographic structure determination of **12** (see below) confirmed the presence of a metal-bound trichlorovinyl ligand *cis* to a chloride ligand, with mutually *trans* triphenylphosphine ligands and mutually *cis* carbonyl ligands.

Synthesis and Reactions of *trans*-Os(Bcat)(Ph)-(CO)₂(PPh₃)₂ (14**) and *trans*-Os(Bcat)(*o*-tolyl)(CO)₂(PPh₃)₂ (**15**).** Carbonylation of the five-coordinate complex **1** produces the expected saturated complex *cis*-Os(Bcat)Cl(CO)₂(PPh₃)₂ (**13**), in which the carbonyl ligands are mutually *cis* and the triphenylphosphine ligands are mutually *trans*. Treatment of **13** with phenyllithium or *o*-tolyllithium produces the *trans* aryl, boryl complexes *trans*-Os(Bcat)(Ph)(CO)₂(PPh₃)₂ (**14**) or *trans*-Os(Bcat)(*o*-tolyl)(CO)₂(PPh₃)₂ (**15**), respectively (see Scheme 5). We have proposed⁴ that this reaction proceeds initially by nucleophilic attack by the aryl anion at the carbonyl ligand *trans* to the Bcat ligand. This is followed by loss of the chloride ligand to form a neutral complex in which the acyl ligand may adopt either an η^1 - or an η^2 -bonding mode. This neutral intermediate then undergoes reverse migratory insertion, placing the aryl ligand *trans* to the boryl ligand. The carbonyl ligand *trans* to the Bcat ligand in **13** is activated toward nucleophilic attack by being located *trans* to the boryl ligand. Other related complexes, viz., *trans*-Ru(Bcat)Cl(CO)₂(PPh₃)₂, *trans*-Os(Bcat)I(CO)₂(PPh₃)₂, Os(Bcat)Cl(CO)(CN-*p*-tolyl)(PPh₃)₂, and Os(Si{OEt}₃)Cl(CO)₂(PPh₃)₂, which contain a carbonyl ligand located *trans* to one of the following ligands, CO, isocyanide, triethoxysilyl, do not show a similar reaction with aryllithium reagents. This emphasizes the specific activating effect of the Bcat ligand. The X-ray crystal structure of **15**⁴ confirms that it is a geometric isomer of **3**.

Because of the *trans* disposition of the boryl and aryl groups, complexes **14** and **15** do not undergo reductive

elimination of aryl-Bcat at room temperature or even when heated under reflux in benzene for several hours. However, under the same conditions but with addition of irradiation with a 1000 W tungsten-halogen lamp, the aryl-Bcat molecule is eliminated and the orthometalated complex $\text{Os}(\text{C}_6\text{H}_4\text{PPh}_2)\text{H}(\text{CO})_2(\text{PPh}_3)$ is formed. Presumably under these conditions the *trans*-isomer must first rearrange to form the *cis*-isomer, which then rapidly undergoes elimination and orthometalation.

Reaction of **15** with I₂ gives an approximately 1:1 mixture of two osmium complexes (Scheme 5), which can be separated easily by column chromatography. The two products, *trans*-Os(Bcat)I(CO)₂(PPh₃)₂ (**16**) and *trans*-Os(*o*-tolyl)I(CO)₂(PPh₃)₂ (**17**), are formed by cleavage of the Os-C(*o*-tolyl) and Os-B bonds, respectively. The *trans* arrangement of the boryl and iodide ligands in **16** was confirmed by X-ray crystallography (see below). Since the corresponding *cis*-isomer was easily accessible, the opportunity was taken to examine the structural parameters, and hence the bonding properties, of the Bcat ligand in these two isomeric complexes. The *cis*-isomer was made by treating Os(Ph)I(CO)(PPh₃)₂ with HBcat to afford Os(Bcat)I(CO)(PPh₃)₂, which in turn reacts with carbon monoxide to form *cis*-Os(Bcat)I(CO)₂(PPh₃)₂ (**18**) (Scheme 6). The structure of **18** was determined by X-ray diffraction analysis. The *trans*-isomer **16** is more thermodynamically stable than the *cis*-isomer **18**, since upon heating under reflux in benzene solution for 2 h, **18** is completely converted to the *trans*-isomer **16**. For octahedral dicarbonyl complexes it is usual to find that the *cis*-dicarbonyl isomer is thermodynamically more stable than the corresponding *trans*-isomer. That this is not so in the above example is once again testimony to the fact that a *trans*-disposition of a Bcat ligand and a π -accepting CO ligand is an unfavorable bonding combination (see later discussion of the structures of **16** and **18**).

Table 2. ^1H NMR Data^a for Ruthenium and Osmium Boryl Complexes and Derived Complexes

complex	^1H , δ (ppm)
<i>cis</i> -Os(Bcat)(<i>o</i> -tolyl)(CO)(CN- <i>p</i> -tolyl)(PPh ₃) ₂ (4) ^b	1.89 (s, 3H, C ₆ H ₄ Me), 2.33 (s, 3H, CNC ₆ H ₄ Me), 6.16–6.63 (m, 5H, C ₆ H ₄ Me, CNC ₆ H ₄ Me), 6.76 (m, 2H, Bcat), 6.82 (m, 2H, Bcat), 7.03–7.39 (m, 33H, PPh ₃ , C ₆ H ₄ Me and CNC ₆ H ₄ Me)
Os(C ₆ H ₄ PPh ₂)H(CO) ₂ (PPh ₃) (5)	– 4.75 (dd, ² J _{HP} = 21.4 Hz, ² J _{HP} = 18.6 Hz, 1H, OsH), 6.63 (m, 1H, OsC ₆ H ₄), 6.87–7.04 (m, 3H, OsC ₆ H ₄), 7.35–7.43 (m, 15H, PPh ₃ and PPh ₂), 7.57–7.66 (m, 8H, PPh ₃ and PPh ₂), 7.88–7.94 (m, 2H, PPh ₂)
Os(C ₆ H ₄ PPh ₂)H(CO)(CN- <i>p</i> -tolyl)(PPh ₃) (6)	Isomer 1: – 5.59 (dd, ² J _{HP} = 20.2 Hz, ² J _{HP} = 17.4 Hz, 1H, OsH), 2.22 (s, 3H, CNC ₆ H ₄ CH ₃), 5.99 (d, ³ J _{HH} = 8.1 Hz, 2H, CNC ₆ H ₄ CH ₃), 6.67 (m, 1H, OsC ₆ H ₄), 6.82 (d, <i>J</i> = 8.1 Hz, 2H, CNC ₆ H ₄ CH ₃) Isomer 2: – 4.58 (dd, ² J _{HP} = 20.8 Hz, ² J _{HP} = 19.2 Hz, 1H, OsH), 2.29 (s, 3H, CNC ₆ H ₄ CH ₃), 6.62 (d, ³ J _{HH} = 8.3 Hz, 2H, CNC ₆ H ₄ CH ₃), 6.74 (m, 1H, OsC ₆ H ₄) Overlapping resonances of both isomers: 6.85–7.24 (m, OsC ₆ H ₄ and CNC ₆ H ₄ CH ₃), 7.29–7.42, 7.63–7.74, 7.98–7.80 (m, PPh ₃ and PPh ₂)
Os(Bcat) ₂ (CO)(CN- <i>p</i> -tolyl)(PPh ₃) ₂ (8)	2.38 (s, 3H, CNC ₆ H ₄ Me), 6.65 (m, 4H, Bcat), 6.78 (m, 4H, Bcat), 6.97 (d, ³ J _{HH} = 8.2 Hz, CNC ₆ H ₄ Me), 7.03 (m, 12H, PPh ₃), 7.11 (m, 8H, PPh ₃ and CNC ₆ H ₄ Me), 7.31–7.35 (m, 12H, PPh ₃)
Os(Bcat)H(CO) ₂ (PPh ₃) ₂ (9)	– 7.18 (t, ² J _{HP} = 21.5 Hz, 1H, OsH), 6.61 (m, 4H, Bcat), 7.20–7.23 (m, 18H, PPh ₃), 7.50–7.56 (m, 12H, PPh ₃)
Ru(Bcat) ₂ (CO) ₂ (PPh ₃) ₂ (10)	6.70 (m, 4H, Bcat), 6.82, (m, 4H, Bcat), 7.09 (m, 12H, PPh ₃), 7.17 (m, 6H, PPh ₃), 7.27–7.33 (m, 12H, PPh ₃)
Ru(Bcat) ₂ (CO)(CN- <i>p</i> -tolyl)(PPh ₃) ₂ (11)	2.38 (s, 3H, CNC ₆ H ₄ Me), 6.65 (m, 4H, Bcat), 6.76 (m, 4H, Bcat), 6.97–7.03 (m, 14H, PPh ₃ and CNC ₆ H ₄ Me), 7.09–7.14 (m, 8H, CNC ₆ H ₄ Me and PPh ₃), 7.32–7.36 (m, 12H, PPh ₃)
Os(CCl=CCl ₂)Cl(CO) ₂ (PPh ₃) ₂ (12)	7.36–7.44 (m, 18H, PPh ₃), 7.57–7.65 (m, 12H, PPh ₃)
<i>cis</i> -Os(Bcat)Cl(CO) ₂ (PPh ₃) ₂ (13)	6.74–6.82 (m, 4H, Bcat), 7.23–7.26 (m, 18H, PPh ₃), 7.61–7.66 (m, 12H, PPh ₃)
<i>trans</i> -Os(Bcat)(Ph)(CO) ₂ (PPh ₃) ₂ (14)	6.62 (m, 2H, Ph), 6.69 (m, 2H, Bcat), 6.75 (m, 3H, Bcat and Ph), 7.09–7.17 (m, 20H, PPh ₃ and Ph), 7.27–7.32 (m, 12H, PPh ₃)
<i>trans</i> -Os(Bcat)I(CO) ₂ (PPh ₃) ₂ (16)	6.61 (m, 2H, Bcat), 6.71 (m, 2H, Bcat), 7.17–7.24 (m, 18H, PPh ₃), 7.61–7.67 (m, 12H, PPh ₃)
<i>cis</i> -Os(Bcat)I(CO) ₂ (PPh ₃) ₂ (18)	6.76–6.82 (m, 4H, Bcat), 7.22–7.24 (m, 18H, PPh ₃), 7.62–7.67 (m, 12H, PPh ₃)
<i>o</i> -tolyl-Bcat	2.74 (s, 3H, C ₆ H ₄ CH ₃), 7.13 (m, 2H, Bcat), 7.28–7.34 (m, 4H, C ₆ H ₄ CH ₃ and Bcat), 7.45 (apparent td, <i>J</i> = 7.7 Hz, <i>J</i> = 1.3 Hz, 1H, C ₆ H ₄ CH ₃), 8.11 (apparent dd, <i>J</i> = 7.7 Hz, <i>J</i> = 1.3 Hz, 1H, C ₆ H ₄ CH ₃)

^a Spectra recorded in CDCl₃ at 25 °C unless indicated otherwise. Chemical shifts are referenced to Me₄Si (δ = 0.00). Splitting patterns and line shapes are indicated thus: s = singlet, d = doublet, t = triplet, q = quartet, br = broad. ^b Recorded at –40 °C.

Crystal Structure Determinations. The crystal structures of complexes **3** and **15** have been reported previously.⁴ In this paper we report crystal structure determinations for complexes **5**, **8**, **10**, **11**, **12**, **16**, and **18**. The crystal and refinement data are presented in Table 5, and selected bond distances and angles for these complexes are presented in Tables 6–12.

Structure of Os(C₆H₄PPh₂)H(CO)₂(PPh₃) (5**).** The molecular structure of **5** is shown in Figure 1. The geometry about osmium is approximately octahedral, with the two phosphorus atoms mutually *trans* and the two carbonyl ligands mutually *cis*. The hydride ligand

was located at an Os–H distance of 1.68(3) Å. Other features of the structure are unremarkable and similar to those of other *ortho*-metalated triphenylphosphine complexes.¹⁰

Structures of the Bis(Bcat) Complexes **8, **10**, and **11**.** The molecular structures of **8**, **10**, and **11** are shown in Figures 2–4. All three compounds have essentially

(10) (a) Bennett, M. A.; Berry, D. E.; Bhargava, S. K.; Ditzel, E. J.; Robertson, G. B.; Willis, A. C. *J. Chem. Soc., Chem. Commun.* **1987**, 1613. (b) Bruce, M. I.; Cifuentes, M. P.; Humphrey, M. G.; Poczman, E.; Snow, M. R.; Tiekink, E. R. T. *J. Organomet. Chem.* **1988**, *338*, 237. (c) Fryzuk, M. D.; Montgomery, C. D.; Rettig, S. J. *Organometallics* **1991**, *10*, 467. (d) Chappell, S. D.; Engelhardt, L. M.; White, A. H.; Raston, C. L. *J. Organomet. Chem.* **1993**, *462*, 295.

Table 3. ^{13}C NMR Data^a for Ruthenium and Osmium Boryl Complexes and Derived Complexes

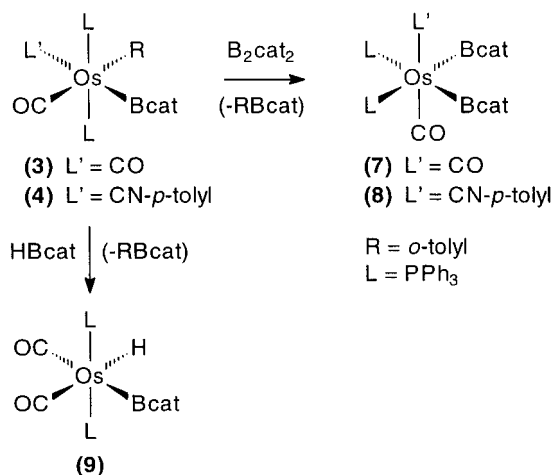
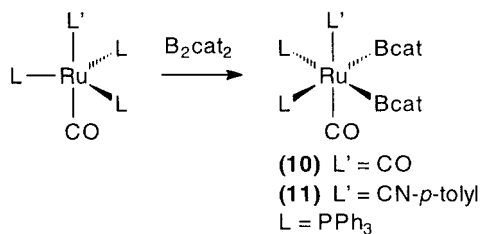
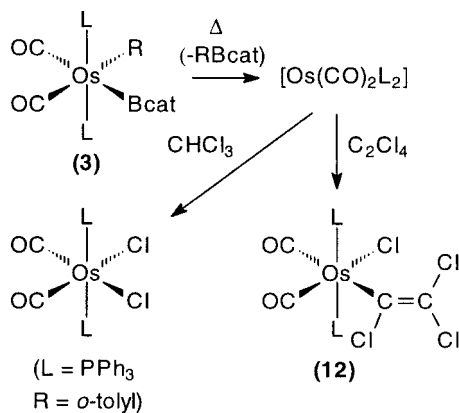
complex	^{13}C , δ (ppm)
<i>cis</i> -Os(Bcat)(<i>o</i> -tolyl)(CO)(CN- <i>p</i> -tolyl)(PPh ₃) ₂ (4) ^d	21.36 (CNC ₆ H ₄ Me), 32.19 (C ₆ H ₄ Me), 110.40 (Bcat), 119.35 (Bcat), 121.73 (C ₆ H ₄ Me), 121.97 (C ₆ H ₄ Me), 124.74 (CNC ₆ H ₄ Me), 126.28 (C ₆ H ₄ Me), 127.08 (t', ^{2,4} J _{CP} = 9 Hz, <i>o</i> -PPh ₃), 128.98 (<i>p</i> -PPh ₃), 129.71 (CNC ₆ H ₄ Me), 133.87 (t', ^{3,5} J _{CP} = 10 Hz, <i>m</i> -PPh ₃), 134.73 (t', ^{1,3} J _{CP} = 50 Hz, <i>i</i> -PPh ₃), 138.05 (CNC ₆ H ₄ Me), 147.79 (t, ² J _{CP} = 11 Hz, <i>i</i> -C ₆ H ₄ Me), 148.24 (C ₆ H ₄ Me), 150.06 (C ₆ H ₄ Me), 150.25 (Bcat), 186.22 (CO) ^{b,c}
Os(C ₆ H ₄ PPh ₂)H(CO) ₂ (PPh ₃) (5)	124.44–139.34 (complex overlapping resonances), 154.46 (dd, ² J _{CP} = 57 Hz, ² J _{CP} = 3 Hz, Os- <i>i</i> -C ₆ H ₄), 183.90 (dd, ² J _{CP} = 7 Hz, ² J _{CP} = 2 Hz, CO), 185.35 (apparent t, ^{2,2} J _{CP} = 6 Hz, CO)
Os(Bcat) ₂ (CO)(CN- <i>p</i> -tolyl)(PPh ₃) ₂ (8)	21.37 (CNC ₆ H ₄ Me), 110.36 (Bcat), 119.52 (Bcat), 125.67 (CNC ₆ H ₄ Me), 127.27 (CNC ₆ H ₄ Me), 127.54 (t', ^{2,4} J _{CP} = 10 Hz, <i>o</i> -PPh ₃), 128.86 (<i>p</i> -PPh ₃), 129.59 (CNC ₆ H ₄ Me), 133.40 (t', ^{3,5} J _{CP} = 12 Hz, <i>m</i> -PPh ₃), 137.52 (m, <i>i</i> -PPh ₃), 138.03 (CNC ₆ H ₄ Me), 150.61 (Bcat), 153.46 (t, ² J _{CP} = 10.5 Hz, CNC ₆ H ₄ Me), 192.16 (t, ² J _{CP} = 7.5 Hz, CO)
Os(Bcat)H(CO) ₂ (PPh ₃) ₂ (9)	110.32 (Bcat), 119.60 (Bcat), 127.76 (t', ^{2,4} J _{CP} = 10 Hz, <i>o</i> -PPh ₃), 129.62 (<i>p</i> -PPh ₃), 133.60 (t', ^{3,5} J _{CP} = 11 Hz, <i>m</i> -PPh ₃), 136.24 (t', ^{1,3} J _{CP} = 53 Hz, <i>i</i> -PPh ₃), 150.13 (Bcat), 186.24 (t, ² J _{CP} = 6 Hz, CO) ^e
Ru(Bcat) ₂ (CO) ₂ (PPh ₃) ₂ (10)	110.74 (Bcat), 120.10 (Bcat), 127.93 (t', ^{2,4} J _{CP} = 8 Hz, <i>o</i> -PPh ₃), 129.24 (<i>p</i> -PPh ₃), 133.16 (t', ^{3,5} J _{CP} = 12 Hz, <i>m</i> -PPh ₃), 136.47 (m, <i>i</i> -PPh ₃), 149.72 (Bcat), 204.21 (t, ² J _{CP} = 9.5 Hz, CO)
Ru(Bcat) ₂ (CO)(CN- <i>p</i> -tolyl)(PPh ₃) ₂ (11)	21.36 (CNC ₆ H ₄ Me), 110.36 (Bcat), 119.55 (Bcat), 125.52 (CNC ₆ H ₄ Me), 127.01 (CNC ₆ H ₄ Me), 127.62 (t', ^{2,4} J _{CP} = 7 Hz, <i>o</i> -PPh ₃), 128.63 (<i>p</i> -PPh ₃), 129.61 (CNC ₆ H ₄ Me), 133.36 (t', ^{3,5} J _{CP} = 12 Hz, <i>m</i> -PPh ₃), 137.65 (m, <i>i</i> -PPh ₃), 138.14 (CNC ₆ H ₄ Me), 150.17 (Bcat), 168.30 (CNC ₆ H ₄ Me), ^c 207.10 (t, ² J _{CP} = 10 Hz, CO)
Os(CCl=CCl ₂)Cl(CO) ₂ (PPh ₃) ₂ (12)	118.91 (t, ³ J _{CP} = 4 Hz, CCl ₂), 127.96 (t', ^{2,4} J _{CP} = 10 Hz, <i>o</i> -PPh ₃), 130.49 (t', ^{1,3} J _{CP} = 52 Hz, <i>i</i> -PPh ₃), 130.69 (<i>p</i> -PPh ₃), 134.39 (t', ^{3,5} J _{CP} = 10 Hz, <i>m</i> -PPh ₃), 143.10 (t, ² J _{CP} = 12.5 Hz, CCl=CCl ₂), 176.06 (t, ² J _{CP} = 8.5 Hz, CO), 179.83 (t, ² J _{CP} = 7.5 Hz, CO)
<i>cis</i> -Os(Bcat)Cl(CO) ₂ (PPh ₃) ₂ (13)	110.93 (Bcat), 120.26 (Bcat), 127.91 (t', ^{2,4} J _{CP} = 10 Hz, <i>o</i> -PPh ₃), 130.05 (<i>p</i> -PPh ₃), 133.32 (t', ^{1,3} J _{CP} = 53 Hz, <i>i</i> -PPh ₃), 133.80 (t', ^{3,5} J _{CP} = 11 Hz, <i>m</i> -PPh ₃), 149.88 (Bcat), 177.87 (t, ² J _{CP} = 7.5 Hz, CO), 182.05 (t, ² J _{CP} = 9 Hz, CO)
<i>trans</i> -Os(Bcat)(Ph)(CO) ₂ (PPh ₃) ₂ (14)	110.09 (Bcat), 119.67 (Bcat), 121.45 (Ph), 127.12 (Ph), 127.49 (t', ^{2,4} J _{CP} = 9 Hz, <i>o</i> -PPh ₃), 129.47 (<i>p</i> -PPh ₃), 133.66 (t', ^{3,5} J _{CP} = 10 Hz, <i>m</i> -PPh ₃), 134.75 (t', ^{1,3} J _{CP} = 52 Hz, <i>i</i> -PPh ₃), 141.25 (t, ² J _{CP} = 9 Hz, <i>i</i> -Ph), 147.16 (Ph), 150.33 (Bcat), 190.30 (t, ² J _{CP} = 11 Hz, CO)
<i>trans</i> -Os(Bcat)I(CO) ₂ (PPh ₃) ₂ (16)	110.57 (Bcat), 120.11 (Bcat), 127.92 (t', ^{2,4} J _{CP} = 10 Hz, <i>o</i> -PPh ₃), 130.11 (<i>p</i> -PPh ₃), 133.71 (t', ^{1,3} J _{CP} = 54 Hz, <i>i</i> -PPh ₃), 133.99 (t', ^{3,5} J _{CP} = 10 Hz, <i>m</i> -PPh ₃), 149.95 (Bcat), 185.14 (t, ² J _{CP} = 10 Hz, CO)
<i>cis</i> -Os(Bcat)I(CO) ₂ (PPh ₃) ₂ (18)	111.02 (Bcat), 120.32 (Bcat), 127.74 (t', ^{2,4} J _{CP} = 10 Hz, <i>o</i> -PPh ₃), 130.02 (<i>p</i> -PPh ₃), 134.03 (t', ^{1,3} J _{CP} = 54 Hz, <i>i</i> -PPh ₃), 134.07 (t', ^{3,5} J _{CP} = 10 Hz, <i>m</i> -PPh ₃), 150.19 (Bcat), 175.12 (t, ² J _{CP} = 7 Hz, CO), 179.45 (t, ² J _{CP} = 9 Hz, CO)
<i>o</i> -tolyl-Bcat	22.44 (C ₆ H ₄ CH ₃), 112.54 (Bcat), 122.70 (Bcat), 125.21 (C ₆ H ₄ CH ₃), 130.32 (C ₆ H ₄ CH ₃), 132.09 (C ₆ H ₄ CH ₃), 136.59 (C ₆ H ₄ CH ₃), 145.57 (C ₆ H ₄ CH ₃), 148.43 (Bcat) ^f

^a Spectra recorded in CDCl₃ at 25 °C unless indicated otherwise. Chemical shifts are referenced to CDCl₃ (δ = 77.00). t' denotes signal has apparent triplet multiplicity, ^{m,n}J_{CP} is the sum of the two coupling constants ^mJ_{CP} and ⁿJ_{CP} as explained in ref 11. ^b CN-*p*-tolyl resonance obscured. ^c Coupling to P not observed. ^d Recorded at -40 °C. ^e Second carbonyl not observed. ^f *ipso*-C₆H₄CH₃ not observed.

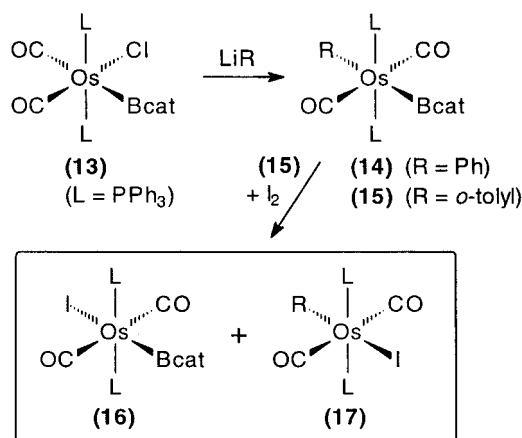
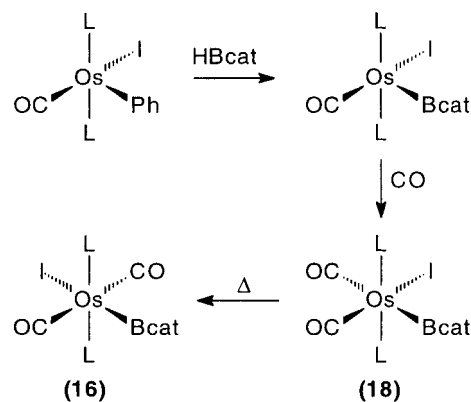
Table 4. ^{11}B NMR Data^a for Selected Boryl Complexes

complex	^{11}B , δ (ppm)
Os(Bcat)(<i>o</i> -tolyl)(CO)(PPh ₃) ₂ (2)	26.5
<i>cis</i> -Os(Bcat)(<i>o</i> -tolyl)(CO) ₂ (PPh ₃) ₂ (3)	46.0
<i>cis</i> -Os(Bcat)(<i>o</i> -tolyl)(CO)(CN- <i>p</i> -tolyl)(PPh ₃) ₂ (4)	47.2
Os(Bcat) ₂ (CO) ₂ (PPh ₃) ₂ (7)	43.9
Os(Bcat) ₂ (CO)(<i>p</i> -CNC ₆ H ₄ Me)(PPh ₃) ₂ (8)	45.6
Os(Bcat)H(CO) ₂ (PPh ₃) ₂ (9)	45.2
Ru(Bcat) ₂ (CO) ₂ (PPh ₃) ₂ (10)	48.2
Ru(Bcat) ₂ (CO)(CN- <i>p</i> -tolyl)(PPh ₃) ₂ (11)	50.0
<i>trans</i> -Os(Bcat)(Ph)(CO) ₂ (PPh ₃) ₂ (14)	43.3
<i>trans</i> -Os(Bcat)(<i>o</i> -tolyl)(CO) ₂ (PPh ₃) ₂ (15)	43.3
<i>trans</i> -Os(Bcat)I(CO) ₂ (PPh ₃) ₂ (16)	36.6 ^b
<i>cis</i> -Os(Bcat)I(CO) ₂ (PPh ₃) ₂ (18)	44.3

^a Spectra recorded in CDCl₃ at 25 °C unless indicated otherwise. Chemical shifts are referenced to BF₃·OEt₂ ($\delta = 0.00$). ^b Spectrum recorded in CDCl₃/CH₂Cl₂.

Scheme 2**Scheme 3****Scheme 4**

the same arrangement of ligands about the metal centers. The two mutually *cis* triphenylphosphine ligands and the two mutually *cis* Bcat ligands are approximately coplanar, with the accompanying two carbonyl (or

Scheme 5**Scheme 6**

carbonyl and isocyanide) ligands occupying axial sites. All metal–phosphorus distances are closely similar as are the P(1)–M–P(2) angles, which range between 103.75(4)° and 109.51(3)°. The M–B bond distances are almost constant over the three compounds (2.086(3)–2.104(6) Å). An interesting feature is that in each case the Bcat ligands are arranged face-to-face with acute B(1)–M–B(2) angles of 77.0(2)°, 75.43(14)°, and 75.57–(12)° for **8**, **10**, and **11**, respectively. Similar small angles have been noted for other bis(boryl) metal complexes.^{2,3} As would be expected, the *cis* triphenylphosphine ligands have P(1)–M–P(2) bond angles greater than 90° and the two carbonyl (or carbonyl and isocyanide) ligands are very close to linear.

Structure of Os(CCl=CCl₂)Cl(CO)(PPh₃)₂ (12**).** The molecular structure of **12** is shown in Figure 5. The geometry about osmium is approximately octahedral with the two phosphorus atoms mutually *trans* and the two carbonyl ligands mutually *cis*. The C(3)–C(4) distance in the trichlorovinyl ligand is 1.293(9) Å, appropriate for a double bond. There is significant variation in the C–Cl distances, the longest being that between the osmium-bound carbon and chloride, i.e., C(4)–Cl(4), which is 1.847(7) Å. The angle Os–C(4)–C(3) is opened considerably from the idealized 120° to 134.2(5)°, while both the angles Os–C(4)–Cl(4) (114.7–(3)°) and C(3)–C(4)–Cl(4) (110.9(5)°) are reduced.

Structures of the Os(Bcat)I(CO)₂(PPh₃)₂ Isomers **16 and **18**.** The molecular structures of *trans*-Os(Bcat)I(CO)₂(PPh₃)₂ (**16**) and *cis*-Os(Bcat)I(CO)₂(PPh₃)₂ (**18**) are shown in Figures 6 and 7, respectively. In both cases the geometry about osmium is approximately octahe-

Table 5. Crystal and Refinement Data for **5**, **8**, **10**, **11**, **12**, **16**, and **18**

	5	8	10	11
formula	C ₃₈ H ₃₀ O ₂ OsP ₂	C ₅₇ H ₄₅ B ₂ O ₅ OsP ₂	C ₅₀ H ₃₈ B ₂ O ₆ P ₂ Ru. C ₇ H ₈	C ₅₇ H ₄₅ B ₂ O ₅ P ₂ Ru
molecular weight	770.76	1097.7	1011.57	1008.57
temp, K	203	203	203	203
wavelength, Å	0.71073	0.71073	0.71073	0.71073
cryst syst	monoclinic	monoclinic	monoclinic	monoclinic
space group	<i>P2₁/n</i>	<i>P2₁/c</i>	<i>P2₁/c</i>	<i>P2₁/c</i>
<i>a</i> , Å	16.35510(10)	10.3198(2)	13.7644(3)	10.3153(3)
<i>b</i> , Å	10.99250(10)	26.6368(4)	19.0556(4)	26.6868(5)
<i>c</i> , Å	17.71080(10)	18.3147(1)	18.7402(1)	18.1026(5)
β, deg	97.350(1)	102.171(1)	94.342(1)	102.177(1)
<i>V</i> , Å ³	3157.92(4)	4872.9(1)	4901.2(9)	4871.2(3)
<i>Z</i>	4	4	4	4
<i>d</i> (calc), g cm ⁻³	1.621	1.496	1.371	1.375
<i>F</i> (000)	1520	2200	2080	2071
μ, mm ⁻¹	4.172	2.733	0.437	0.438
cryst size, mm	0.40 × 0.37 × 0.26	0.35 × 0.11 × 0.11	0.57 × 0.47 × 0.11	0.36 × 0.10 × 0.08
2θ (min – max), deg	1.6–27.1	1.4–27.5	1.5–28.3	1.4–28.2
<i>h, k, l</i> range	–20 ≤ <i>h</i> ≤ 20, 0 ≤ <i>k</i> ≤ 14, 0 ≤ <i>l</i> ≤ 22	–13 ≤ <i>h</i> ≤ 13, 0 ≤ <i>k</i> ≤ 34, 0 ≤ <i>l</i> ≤ 23	–18 ≤ <i>h</i> ≤ 17, 0 ≤ <i>k</i> ≤ 24, 0 ≤ <i>l</i> ≤ 23	–12 ≤ <i>h</i> ≤ 12, 0 ≤ <i>k</i> ≤ 34, 0 ≤ <i>l</i> ≤ 22
no. of reflns collected	18 839	28 732	28 827	29 954
no. of independent reflns	6764, <i>R</i> _{int} 0.0189	10 623, <i>R</i> _{int} 0.0526	10 975, <i>R</i> _{int} 0.0326	10 908, <i>R</i> _{int} 0.0405
<i>A</i> (min, max)	0.2861, 0.4101	0.448, 0.753	0.789, 0.953	0.858, 0.966
function minimized	Σ <i>w</i> (<i>F</i> _o ² – <i>F</i> _c ²) ²	Σ <i>w</i> (<i>F</i> _o ² – <i>F</i> _c ²) ²	Σ <i>w</i> (<i>F</i> _o ² – <i>F</i> _c ²) ²	Σ <i>w</i> (<i>F</i> _o ² – <i>F</i> _c ²) ²
no. of data/restraints/params	6764/0/391	10 623/0/614	10 975/0/578	10 908/0/614
goodness of fit on <i>F</i> ²	1.060	1.096	0.949	1.072
<i>R</i> (obsd data) ^a	<i>R</i> 1 = 0.0222 w <i>R</i> 2 = 0.0545	<i>R</i> 1 = 0.0481 w <i>R</i> 2 = 0.0698	<i>R</i> 1 = 0.0400 w <i>R</i> 2 = 0.0926	<i>R</i> 1 = 0.0416 w <i>R</i> 2 = 0.0678
<i>R</i> (all data)	<i>R</i> 1 = 0.0251 w <i>R</i> 2 = 0.0565	<i>R</i> 1 = 0.0869 w <i>R</i> 2 = 0.0836	<i>R</i> 1 = 0.0693 w <i>R</i> 2 = 0.11104	<i>R</i> 1 = 0.0737 w <i>R</i> 2 = 0.0788
least-squares weights <i>a, b</i>	0.0230, 5.2423	0.0000, 11.605	0.0538, 4.893	0.0111, 3.860
diff map (min, max), e Å ⁻³	+1.76, –0.91	+0.99, –0.99	+0.59, –0.56	+0.37, –0.43

	12	16	18
formula	C ₄₀ H ₃₀ Cl ₄ O ₂ OsP ₂	C ₄₄ H ₃₄ BIO ₄ OsP ₂ .CH ₂ Cl ₂	C ₄₄ H ₃₄ BIO ₄ OsP ₂ .CH ₂ Cl ₂
molecular weight	936.58	1101.49	1101.49
temp, K	203	203	203
wavelength, Å	0.71073	0.71073	0.71073
cryst syst	orthorhombic	monoclinic	orthorhombic
space group	<i>Pbca</i>	<i>P2₁/c</i>	<i>P2₁2₁2₁</i>
<i>a</i> , Å	12.0712(1)	17.0528(2)	11.2964(1)
<i>b</i> , Å	17.2622(1)	13.2932(1)	11.9060(1)
<i>c</i> , Å	34.6301(1)	19.4297(2)	31.3608(3)
β, deg		109.013(1)	
<i>V</i> , Å ³	7216.06(8)	4274.05(7)	4217.97(5)
<i>Z</i>	8	4	14
<i>d</i> (calc) g cm ⁻³	1.724	1.712	1.735
<i>F</i> (000)	3680	2144	2144
μ, mm ⁻¹	3.955	3.948	4.000
cryst size, mm	0.42 × 0.21 × 0.13	0.38 × 0.30 × 0.30	0.55 × 0.36 × 0.27
2θ (min, max) deg.	2.1, 27.2	1.9, 28.3	1.3, 26.5
<i>h, k, l</i> range	0 ≤ <i>h</i> ≤ 15, 0 ≤ <i>k</i> ≤ 21, 0 ≤ <i>l</i> ≤ 44	–23 ≤ <i>h</i> ≤ 21, 0 ≤ <i>k</i> ≤ 17, 0 ≤ <i>l</i> ≤ 25	–14 ≤ <i>h</i> ≤ 14, 0 ≤ <i>k</i> ≤ 24, 0 ≤ <i>l</i> ≤ 39
no. of reflns collected	43 497	25 972	23 823
no. of ind reflns	7861, <i>R</i> _{int} 0.0255	9540, <i>R</i> _{int} 0.0152	8615, <i>R</i> _{int} 0.0394
<i>A</i> (min, max)	0.287, 0.627	0.315, 0.383	0.217, 0.411
function minimized	Σ <i>w</i> (<i>F</i> _o ² – <i>F</i> _c ²) ²	Σ <i>w</i> (<i>F</i> _o ² – <i>F</i> _c ²) ²	Σ <i>w</i> (<i>F</i> _o ² – <i>F</i> _c ²) ²
no. of data/restraints/params	7861/0/442	9540/0/500	8615/0/506
goodness of fit on <i>F</i> ²	1.393	1.104	1.015
<i>R</i> (obsd data)	<i>R</i> 1 = 0.0434 w <i>R</i> 2 = 0.0902	<i>R</i> 1 = 0.0207 w <i>R</i> 2 = 0.0540	<i>R</i> 1 = 0.0249 w <i>R</i> 2 = 0.0547
<i>R</i> (all data)	<i>R</i> 1 = 0.0468 w <i>R</i> 2 = 0.0914	<i>R</i> 1 = 0.0228 w <i>R</i> 2 = 0.0553	<i>R</i> 1 = 0.0276 w <i>R</i> 2 = 0.0560
least-squares weights <i>a, b</i>	0.0000, 49.27	0.0235, 6.110	0.0000, 0.1000
diff map (min, max), e Å ⁻³	+1.47, –2.15	+1.18, –0.83	+0.89, –0.77

$$^a R = \sum |F_o| - |F_c| / \sum |F_o|. \text{wR2} = \{ \sum [w(F_o^2 - F_c^2)^2] / \sum [w(F_o^2)^2] \}^{1/2}. \text{Weight} = 1.0 / [\sigma^2(F_o^2) + aP^2 + bP]; P = (F_o^2 + 2F_c^2) / 3.$$

dral, with the two phosphorus atoms mutually *trans* and the two carbonyl ligands either mutually *trans* (**16**) or *cis* (**18**). In complex **16** the boryl ligand is located *trans* to the iodide ligand and a strong *trans* influence is apparent from a long Os–I bond distance of 2.8346(2) Å. The carbonyl ligands are displaced toward the Bcat

ligand (angle C(1)–Os–B, 84.85(12)° and angle C(2)–Os–B, 82.60(12)°), and the orientation of the plane of the Bcat ligand is tilted by 11.83(13)° with respect to the plane of best fit through the Os, B, C(1), C(2), and I atoms. The average Os–CO bond distance is 1.941(3) Å and the Os–B bond distance is 2.090(3) Å, much

Table 6. Selected Bond Distances (Å) and Angles (deg) for Complex 5

Interatomic Distances			
Os–H(1)	1.68(3)	O(2)–C(2)	1.153(4)
Os–C(2)	1.908(3)	C(11)–C(16)	1.396(4)
Os–C(1)	1.943(3)	C(11)–C(12)	1.420(4)
Os–C(12)	2.166(3)	C(12)–C(13)	1.405(4)
Os–P(1)	2.3512(7)	C(13)–C(14)	1.397(4)
Os–P(2)	2.3637(7)	C(14)–C(15)	1.387(5)
O(1)–C(1)	1.141(4)	C(15)–C(16)	1.388(5)
Interatomic Angles			
H(1)–Os–C(2)	85.4(11)	C(31)–P(1)–C(21)	104.86(13)
H(1)–Os–C(1)	176.4(11)	C(11)–P(1)–Os	87.64(9)
C(2)–Os–C(1)	96.47(13)	C(31)–P(1)–Os	119.21(9)
H(1)–Os–C(12)	86.1(11)	C(21)–P(1)–Os	122.26(10)
C(2)–Os–C(12)	168.24(12)	O(1)–C(1)–Os	174.8(3)
C(1)–Os–C(12)	91.68(11)	O(2)–C(2)–Os	177.9(3)
H(1)–Os–P(1)	86.7(11)	C(16)–C(11)–C(12)	123.4(3)
C(2)–Os–P(1)	105.15(9)	C(16)–C(11)–P(1)	137.0(2)
C(1)–Os–P(1)	89.82(8)	C(12)–C(11)–P(1)	99.58(19)
C(12)–Os–P(1)	66.28(8)	C(13)–C(12)–C(11)	116.5(3)
H(1)–Os–P(2)	85.5(11)	C(13)–C(12)–Os	137.3(2)
C(2)–Os–P(2)	92.49(9)	C(11)–C(12)–Os	106.27(19)
C(1)–Os–P(2)	97.46(8)	C(14)–C(13)–C(12)	120.2(3)
C(12)–Os–P(2)	94.86(8)	C(15)–C(14)–C(13)	121.6(3)
P(1)–Os–P(2)	160.07(3)	C(16)–C(15)–C(14)	120.2(3)
C(11)–P(1)–C(31)	111.53(13)	C(15)–C(16)–C(11)	118.0(3)
C(11)–P(1)–C(21)	109.88(14)		

Table 7. Selected Bond Distances (Å) and Angles (deg) for Complex 8

Interatomic Distances			
Os–B(1)	2.104(6)	C(1)–O(1)	1.160(5)
Os–B(2)	2.093(6)	C(2)–N	1.162(6)
Os–C(1)	1.892(5)	B(1)–O(2)	1.434(7)
Os–C(14)	1.986(5)	B(1)–O(3)	1.422(7)
Os–P(1)	2.4134(12)	B(2)–O(4)	1.439(6)
Os–P(2)	2.4305(13)	B(2)–O(5)	1.428(6)
Interatomic Angles			
C(1)–Os–B(1)	85.2(2)	P(1)–Os–P(2)	103.75(4)
C(1)–Os–B(2)	85.9(2)	P(1)–Os–B(1)	166.32(17)
C(1)–Os–C(2)	171.0(2)	P(1)–Os–B(2)	90.82(15)
C(1)–Os–P(1)	87.77(15)	P(2)–Os–B(1)	88.95(16)
C(1)–Os–P(2)	99.03(15)	P(2)–Os–B(2)	164.73(15)
C(2)–Os–B(1)	92.1(2)	B(1)–Os–B(2)	77.0(2)
C(2)–Os–B(2)	85.1(2)	O(1)–C(1)–Os	176.4(4)
C(2)–Os–P(1)	93.12(14)	N–C(2)–Os	178.5(4)
C(2)–Os–P(2)	89.49(14)		

Table 8. Selected Bond Distances (Å) and Angles (deg) for Complex 10

Interatomic Distances			
Ru–B(1)	2.100(3)	C(1)–O(1)	1.143(4)
Ru–B(2)	2.095(4)	C(2)–O(2)	1.140(4)
Ru–C(1)	1.919(3)	B(1)–O(3)	1.412(4)
Ru–C(2)	1.914(3)	B(1)–O(4)	1.404(4)
Ru–P(1)	2.4508(8)	B(2)–O(5)	1.417(4)
Ru–P(2)	2.4583(9)	B(2)–O(6)	1.409(4)
Interatomic Angles			
C(1)–Ru–B(1)	86.01(13)	P(1)–Ru–P(2)	109.51(3)
C(1)–Ru–B(2)	86.94(15)	P(1)–Ru–B(1)	162.46(10)
C(1)–Ru–C(2)	171.09(14)	P(1)–Ru–B(2)	87.59(10)
C(1)–Ru–P(1)	97.64(10)	P(2)–Ru–B(1)	87.65(10)
C(1)–Ru–P(2)	88.65(11)	P(2)–Ru–B(2)	162.76(10)
C(2)–Ru–B(1)	87.25(13)	B(1)–Ru–B(2)	75.43(14)
C(2)–Ru–B(2)	85.73(14)	O(1)–C(1)–Ru	177.2(3)
C(2)–Ru–P(1)	87.12(10)	O(2)–C(2)–Ru	176.8(3)
C(2)–Ru–P(2)	96.90(10)		

shorter than the Os–B bond distance for the *cis* isomer (see below).

In complex **18**, despite being *trans* to a carbonyl ligand, the Os–I bond length is 2.7883(3) Å, a distance that is much shorter than that found in **16**. Also, the

Table 9. Selected Bond Distances (Å) and Angles (deg) for Complex 11

Interatomic Distances			
Ru–B(1)	2.093(3)	C(1)–O(1)	1.146(3)
Ru–B(2)	2.086(3)	C(2)–N(1)	1.164(3)
Ru–C(1)	1.890(3)	B(1)–O(2)	1.427(4)
Ru–C(2)	1.987(3)	B(1)–O(3)	1.418(4)
Ru–P(1)	2.4255(7)	B(2)–O(4)	1.424(4)
Ru–P(2)	2.4438(7)	B(2)–O(5)	1.421(4)
Interatomic Angles			
C(1)–Ru–B(1)	85.25(13)	P(1)–Ru–P(2)	104.00(3)
C(1)–Ru–B(2)	85.55(12)	P(1)–Ru–B(1)	165.69(9)
C(1)–Ru–C(2)	170.52(11)	P(1)–Ru–B(2)	91.50(9)
C(1)–Ru–P(1)	87.69(9)	P(2)–Ru–B(1)	89.45(9)
C(1)–Ru–P(2)	99.45(9)	P(2)–Ru–B(2)	163.83(9)
C(2)–Ru–B(1)	91.56(12)	B(1)–Ru–B(2)	75.57(12)
C(2)–Ru–B(2)	85.01(12)	O(1)–C(1)–Ru	176.1(3)
C(2)–Ru–P(1)	93.41(8)	N(1)–C(2)–Ru	178.5(2)
C(2)–Ru–P(2)	89.43(8)		

Table 10. Selected Bond Distances (Å) and Angles (deg) for Complex 12

Interatomic Distances			
Os–C(1)	1.901(8)	Cl(2)–C(3)	1.707(8)
Os–C(2)	1.941(6)	Cl(4)–C(4)	1.847(7)
Os–C(4)	2.151(6)	Cl(3)–C(3)	1.768(7)
Os–P(2)	2.4421(14)	O(1)–C(1)	1.034(8)
Os–P(1)	2.4477(14)	O(2)–C(2)	1.128(7)
Os–Cl(1)	2.4757(16)	C(3)–C(4)	1.293(9)
Interatomic Angles			
C(1)–Os–C(2)	93.(2)	C(4)–Os–Cl(1)	92.22(18)
C(1)–Os–C(4)	94.4(2)	P(2)–Os–Cl(1)	84.89(5)
C(2)–Os–C(4)	172.3(3)	P(1)–Os–Cl(1)	95.83(5)
C(1)–Os–P(2)	94.22(18)	O(1)–C(1)–Os	175.2(6)
C(2)–Os–P(2)	88.78(17)	O(2)–C(2)–Os	174.6(5)
C(4)–Os–P(2)	92.57(16)	C(4)–C(3)–Cl(2)	121.9(5)
C(1)–Os–P(1)	85.13(18)	C(4)–C(3)–Cl(3)	126.7(6)
C(2)–Os–P(1)	91.84(17)	Cl(2)–C(3)–Cl(3)	111.3(4)
C(4)–Os–P(1)	86.89(16)	C(3)–C(4)–Cl(4)	110.9(5)
P(2)–Os–P(1)	179.12(5)	C(3)–C(4)–Os	134.2(5)
C(1)–Os–Cl(1)	173.31(18)	Cl(4)–C(4)–Os	114.7(3)
C(2)–Os–Cl(1)	80.39(18)		

Table 11. Selected Bond Distances (Å) and Angles (deg) for Complex 16

Interatomic Distances			
Os–B	2.090(3)	Os–P(2)	2.3821(6)
Os–C(1)	1.938(3)	C(1)–O(1)	1.137(3)
Os–C(2)	1.944(3)	C(2)–O(2)	1.130(3)
Os–I	2.8346(2)	B–O(3)	1.415(3)
Os–P(1)	2.3995(6)	B–O(4)	1.410(4)
Interatomic Angles			
C(1)–Os–B	84.85(12)	P(1)–Os–P(2)	178.19(2)
C(1)–Os–C(2)	166.93(12)	P(1)–Os–I	88.656(16)
C(1)–Os–I	98.68(8)	P(1)–Os–B	89.65(8)
C(1)–Os–P(1)	90.01(8)	P(2)–Os–I	92.493(16)
C(1)–Os–P(2)	88.53(8)	P(2)–Os–B	91.30(8)
C(2)–Os–B	82.60(12)	I–Os–B	174.88(8)
C(2)–Os–I	94.09(8)	O(1)–C(1)–Os	173.6(3)
C(2)–Os–P(1)	93.54(8)	O(2)–C(2)–Os	173.8(3)
C(2)–Os–P(2)	88.12(8)		

Os–CO bond distance for the carbonyl ligand *trans* to the Bcat ligand is significantly longer (1.968(5) Å) than the Os–CO bond distance for the carbonyl ligand which is *trans* to the iodide ligand (1.867(4) Å) and longer even than the Os–CO bond distances for the mutually *trans* CO ligands in **16**. These observations are consistent with the Bcat ligand having a large *trans* influence and considerable π -acceptor character. In **18**, where Bcat and CO are *trans* to one another, the Os–B bond distance (2.145(5) Å) is much longer than the corresponding distance in **16** (2.090(3) Å). This further

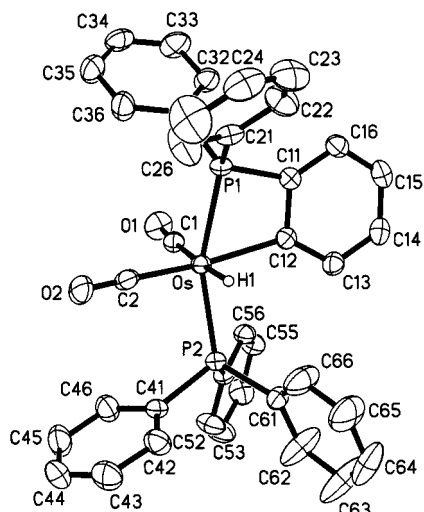


Figure 1. Molecular structure of $\text{Os}(\text{C}_6\text{H}_4\text{PPh}_2)\text{H}(\text{CO})_2(\text{PPh}_3)$ (**5**) with thermal ellipsoids at the 50% probability level.

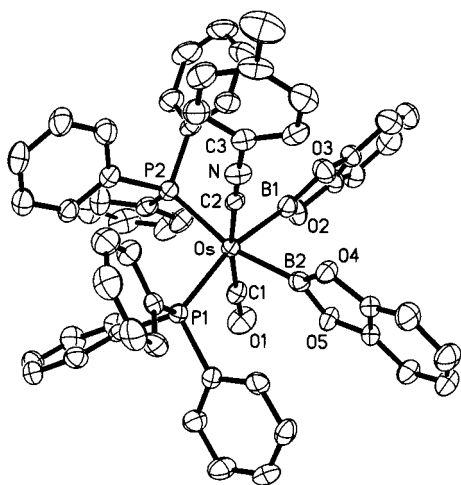


Figure 2. Molecular structure of $\text{Os}(\text{Bcat})_2(\text{CO})(\text{CN-}p\text{-tolyl})(\text{PPh}_3)_2$ (**8**) with thermal ellipsoids at the 50% probability level.

Table 12. Selected Bond Distances (Å) and Angles (deg) for Complex 18

Interatomic Distances			
Os–B	2.145(5)	Os–P(2)	2.3972(10)
Os–C(1)	1.867(4)	C(1)–O(1)	1.155(5)
Os–C(2)	1.968(5)	C(2)–O(2)	1.094(5)
Os–I	2.7883(3)	B–O(3)	1.419(5)
Os–P(1)	2.3934(10)	B–O(4)	1.408(5)
Interatomic Angles			
C(1)–Os–B	84.52(18)	P(1)–Os–P(2)	175.68(4)
C(1)–Os–C(2)	93.85(17)	P(1)–Os–I	88.84(2)
C(1)–Os–I	170.37(13)	P(1)–Os–B	88.47(12)
C(1)–Os–P(1)	90.46(12)	P(2)–Os–I	88.17(2)
C(1)–Os–P(2)	91.97(12)	P(2)–Os–B	88.20(12)
C(2)–Os–B	178.35(17)	I–Os–B	85.87(12)
C(2)–Os–I	95.76(12)	O(1)–C(1)–Os	178.1(4)
C(2)–Os–P(1)	91.34(12)	O(2)–C(2)–Os	173.6(4)
C(2)–Os–P(2)	92.06(12)		

supports the notion that the Bcat ligand is behaving as a π -acceptor ligand, which in this position is in competition with CO. Both the iodide and the carbonyl ligand *cis* to Bcat in **18** are slightly displaced toward the boryl ligand at angles of 85.87(12)° and 84.52(18)°, respectively, and the orientation of the plane of the Bcat ligand

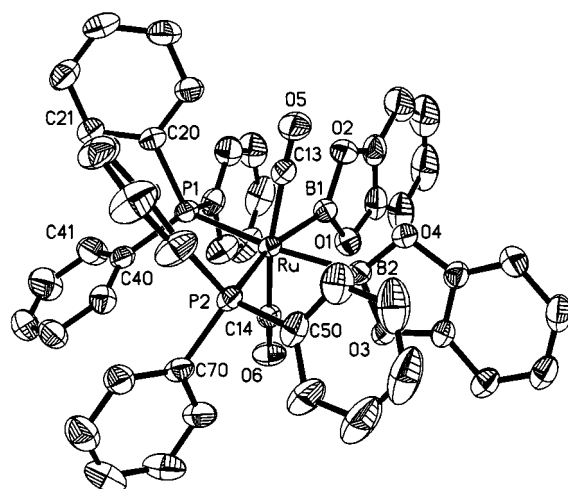


Figure 3. Molecular structure of $\text{Ru}(\text{Bcat})_2(\text{CO})_2(\text{PPh}_3)_2$ (**10**) with thermal ellipsoids at the 50% probability level.

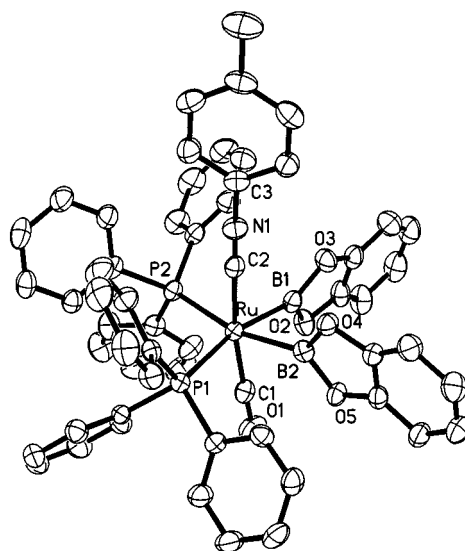


Figure 4. Molecular structure of $\text{Ru}(\text{Bcat})_2(\text{CO})(\text{CN-}p\text{-tolyl})(\text{PPh}_3)_2$ (**11**) with thermal ellipsoids at the 50% probability level.

is tilted by 2.41(8)° with respect to the plane of best fit through the Os, B, C(1), C(2), and I atoms.

Conclusions

The successful synthesis and characterization of compounds with either *cis* or *trans* arrangements of Os–B and Os–C(aryl) reveals that the *cis* arrangement readily undergoes reductive elimination of organoborane, thus verifying theoretical predictions. In contrast the *trans* isomer is stable in this respect. The elimination process offers a simple route to four-coordinate osmium(0) complexes which have been trapped through oxidative addition reactions involving B–H, B–B, and C–Cl bonds. In the absence of trapping reagents *ortho*-metalation of one of the triphenylphosphine phenyl rings occurs. Many of these products have been structurally characterized, including a novel pair of geometrical isomers, *cis*- and *trans*-Os(Bcat)I(CO)₂(PPh₃)₂. The structural parameters of these two compounds indicate that the Bcat ligand has significant π -acceptor character. This conclusion is further supported by the thermal isomerization of *cis*-Os(Bcat)I(CO)₂(PPh₃)₂ (where

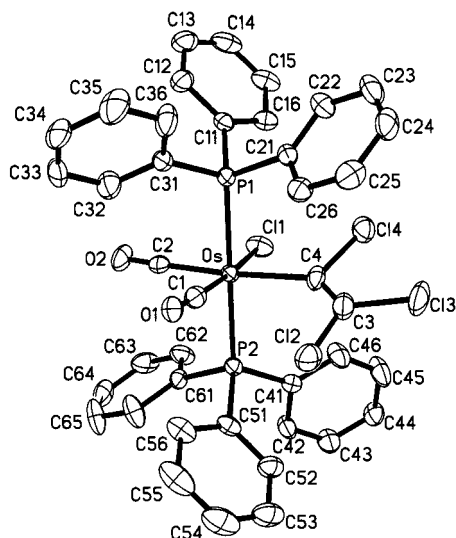


Figure 5. Molecular structure of $\text{OsCl}(\text{CCl}=\text{CCl}_2)(\text{CO})_2(\text{PPh}_3)_2$ (**12**) with thermal ellipsoids at the 50% probability level.

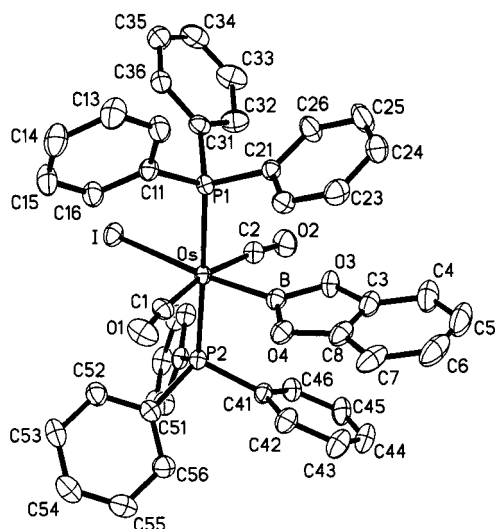


Figure 6. Molecular structure of $\text{trans-Os}(\text{Bcat})\text{I}(\text{CO})_2(\text{PPh}_3)_2$ (**16**) with thermal ellipsoids at the 50% probability level.

Bcat is *trans* to CO) to $\text{trans-Os}(\text{Bcat})\text{I}(\text{CO})_2(\text{PPh}_3)_2$ (where Bcat is *trans* to I and the two CO ligands are mutually *trans*).

Experimental Section

General Considerations. The general experimental and spectroscopic techniques employed in this work were the same as those described previously.¹¹ $\text{Os}(\text{Bcat})\text{Cl}(\text{CO})(\text{PPh}_3)_2$,⁵ $\text{Os}(\text{Bcat})(o\text{-tolyl})(\text{CO})(\text{PPh}_3)_2$,⁴ $\text{trans-Os}(\text{Bcat})(o\text{-tolyl})(\text{CO})_2(\text{PPh}_3)_2$,⁴ $\text{Ru}(\text{CO})_2(\text{PPh}_3)_3$,¹² and $\text{Ru}(\text{CO})(\text{CN-}p\text{-tolyl})(\text{PPh}_3)_3$ ¹³ were prepared as reported previously.

Infrared spectra ($4000\text{--}400\text{ cm}^{-1}$) were recorded as Nujol mulls between KBr plates on a Perkin-Elmer Paragon 1000 spectrometer. NMR spectra were obtained on a Bruker DRX 400 at 25 °C. ¹H, ¹³C, ¹¹B, and ³¹P NMR spectra were obtained operating at 400.1 (¹H), 100.6 (¹³C), 128.0 (¹¹B), and 162.0 (³¹P)

(11) Maddock, S. M.; Rickard, C. E. F.; Roper, W. R.; Wright, L. J. *Organometallics* **1996**, *15*, 1793.

(12) Cavit, B. E.; Grundy, K. R.; Roper, W. R. *J. Chem. Soc., Chem. Commun.* **1972**, 60.

(13) Christian, D. F.; Clark, G. R.; Roper, W. R.; Waters, J. M.; Whittle, K. R. *J. Chem. Soc., Chem. Commun.* **1972**, 458.

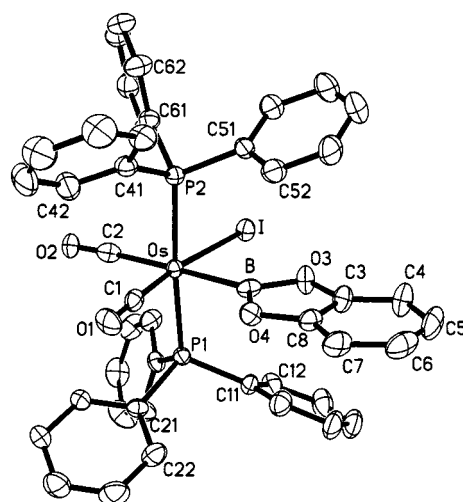


Figure 7. Molecular structure of $\text{cis-Os}(\text{Bcat})\text{I}(\text{CO})_2(\text{PPh}_3)_2$ (**18**) with thermal ellipsoids at the 50% probability level.

MHz, respectively. Resonances are quoted in ppm and ¹H NMR spectra referenced to either tetramethylsilane (0.00 ppm) or the proteo impurity in the solvent (7.25 ppm for CHCl_3). ¹³C NMR spectra were referenced to CDCl_3 (77.00 ppm), ³¹P NMR spectra to 85% orthophosphoric acid (0.00 ppm) as an external standard, and ¹¹B NMR spectra to $\text{BF}_3\cdot\text{OEt}_2$ as an external standard. Mass spectra were recorded with a Varian VG 70-SE mass spectrometer. Elemental analyses were obtained from the Microanalytical Laboratory, University of Otago.

cis-Os(Bcat)(o-tolyl)(CO)(CN-*p*-tolyl)(PPh₃)₂ (**4**). A solution of *p*-tolylisocyanide (37 mg, 0.32 mmol) in benzene was added to a solution of $\text{Os}(\text{Bcat})(o\text{-tolyl})(\text{CO})(\text{PPh}_3)_2$ (252 mg, 0.264 mmol) in benzene (20 mL), whereupon the mixture became a pale yellow color. The solution was concentrated to ca. 1 mL in vacuo and hexane then added to give pure **4** as a white microcrystalline solid, which was collected on a glass frit and washed with EtOH and hexane (yield 256 mg, 90%). Anal. Calcd for $\text{C}_{58}\text{H}_{48}\text{BNO}_3\text{OsP}_2$: C, 65.11; H, 4.52. Found: C, 65.20; H, 4.31.

$\text{Os}(\text{C}_6\text{H}_4\text{PPh}_2)\text{H}(\text{CO})_2(\text{PPh}_3)$ (**5**). A solution of $\text{cis-Os}(\text{Bcat})(o\text{-tolyl})(\text{CO})_2(\text{PPh}_3)_2$ (151 mg, 0.154 mmol) in benzene (10 mL) was stirred at 20 °C for 16 h. The resulting solution was filtered, and the benzene was then removed in vacuo. The solid residue was recrystallized from $\text{CH}_2\text{Cl}_2/\text{EtOH}$ to give pure **5** as a white microcrystalline solid, which was collected on a glass frit and washed with EtOH and hexane (yield 95 mg, 80%). ³¹P NMR (CDCl_3): δ -65.58 (d, ²*J*_{PP} = 218 Hz), 13.95 (d, ²*J*_{PP} = 217 Hz). Anal. Calcd for $\text{C}_{38}\text{H}_{30}\text{O}_2\text{OsP}_2$: C, 59.21; H, 3.92. Found: C, 59.17; H, 3.82.

***o*-tolylBcat.** The filtrate obtained in the recrystallization of **5** from $\text{CH}_2\text{Cl}_2/\text{EtOH}$ above was dissolved in light petroleum and filtered. The solvent was then removed in vacuo to give crude *o*-tolyl-Bcat as a white solid. It was not possible to completely purify the sample, and hence acceptable elemental analysis was not obtained. The compound was characterized by ¹H and ¹³C NMR spectroscopy (see Tables 2 and 3), ¹¹B NMR spectroscopy (CDCl_3 , δ , 32.3 ppm), and mass spectrometry, which showed a prominent signal corresponding to the molecular ion (EI⁺, *m/z* = 210).

$\text{Os}(\text{C}_6\text{H}_4\text{PPh}_2)\text{H}(\text{CO})(\text{CN-}p\text{-tolyl})(\text{PPh}_3)$ (**6a** and **6b**). A solution of $\text{cis-Os}(\text{Bcat})(o\text{-tolyl})(\text{CO})(\text{CN-}p\text{-tolyl})(\text{PPh}_3)_2$ (87 mg, 0.081 mmol) in benzene (10 mL) was stirred at 20 °C for 16 h. The resulting cloudy solution was filtered through Celite, and the benzene was then removed in vacuo. The resulting solid residue was recrystallized from $\text{CH}_2\text{Cl}_2/\text{EtOH}$ to give **6** as a pale yellow microcrystalline solid, which was collected on a glass frit and washed quickly with hexane (yield 34 mg, 49%). The product could not be obtained in highly pure form due to

its high solubility in organic solvents. ^1H and ^{31}P NMR spectroscopy showed that the product exists as two isomers in a ratio of approximately 2:1. ^{31}P NMR (CDCl_3) major isomer: δ -62.46 (d, $^2J_{\text{PP}} = 232$ Hz), 16.50 (d, $^2J_{\text{PP}} = 232$ Hz). Minor isomer: δ -63.59 (d, $J_{\text{PP}} = 230$ Hz), 17.29 (d, $J_{\text{PP}} = 230$ Hz). Anal. Calcd for $\text{C}_{45}\text{H}_{37}\text{NO}_5\text{OsP}_2$: C, 62.85; H, 4.34; N, 1.63. Found: C, 61.85; H, 4.43; N, 1.50.

Os(Bcat) $_2$ (CO)(CN-*p*-tolyl)(PPh $_3$) $_2$ (8). A mixture of *cis*-Os(Bcat)(*o*-tolyl)(CO)(CN-*p*-tolyl)(PPh $_3$) $_2$ (104 mg, 0.0972 mmol) and B_2cat_2 (46 mg, 0.19 mmol) was dissolved in benzene (12 mL), and the colorless solution was stirred at 20 °C for 16 h. The benzene was removed in vacuo from the resulting pale yellow solution, and then CH_2Cl_2 (10 mL) was added to the solid residue. The resulting suspension was filtered through Celite, and EtOH (5 mL) was added to the filtrate. The CH_2Cl_2 was removed in vacuo to give pure **8** as a white microcrystalline solid, which was collected on a glass frit and washed with EtOH and hexane (yield 92 mg, 86%). Anal. Calcd for $\text{C}_{57}\text{H}_{45}\text{B}_2\text{NO}_5\text{OsP}_2$: C, 62.37; H, 4.13; N, 1.28. Found: C, 62.10; H, 4.08; N, 1.49.

Os(Bcat)H(CO) $_2$ (PPh $_3$) $_2$ (9). A mixture of *cis*-Os(Bcat)(*o*-tolyl)(CO) $_2$ (PPh $_3$) $_2$ (106 mg, 0.108 mmol) and HBcat (0.020 mL, 0.19 mmol) was dissolved in benzene (12 mL), and the colorless solution was stirred at 20 °C for 16 h. The benzene was removed in vacuo from the resulting orange suspension, and then CH_2Cl_2 (10 mL) was added to the solid residue. The resulting suspension was filtered through Celite, and EtOH (5 mL) was added to the filtrate. Removal of the CH_2Cl_2 in vacuo gave **9** as a white microcrystalline solid, which was collected on a glass frit and washed with EtOH and hexane (yield 90 mg, 93%). Anal. Calcd for $\text{C}_{44}\text{H}_{35}\text{BO}_4\text{OsP}_2$: C, 59.33; H, 3.96. Found: C, 59.11; H, 3.78.

Ru(Bcat) $_2$ (CO) $_2$ (PPh $_3$) $_2$ (10). A mixture of $\text{Ru}(\text{CO})_2(\text{PPh}_3)_3$ (200 mg, 0.212 mmol) and B_2cat_2 (62 mg, 0.26 mmol) was dissolved in toluene (15 mL), and the yellow solution was irradiated for 5 min by a 1000 W tungsten-halogen lamp held 10 cm from the flask. The solution was then stirred at 20 °C for 1.5 h without irradiation. The solvent was removed in vacuo from the resulting pale yellow solution, and CH_2Cl_2 (10 mL) was added to the solid residue. Addition of EtOH (10 mL) and removal of the CH_2Cl_2 in vacuo gave pure **10** as a white microcrystalline solid, which was collected on a glass frit and washed with EtOH and hexane (yield 97 mg, 50%). X-ray diffraction analysis confirmed 1 equiv of toluene present as solvate in the single crystal used for the X-ray analysis. Anal. Calcd for $\text{C}_{50}\text{H}_{38}\text{B}_2\text{O}_6\text{P}_2\text{Ru}\cdot\text{C}_7\text{H}_8$: C, 67.68; H, 4.58. Found: C, 67.73; H, 4.52.

Ru(Bcat) $_2$ (CO)(CN-*p*-tolyl)(PPh $_3$) $_2$ (11). A mixture of $\text{Ru}(\text{CO})(\text{CN-}i\text{-}p\text{-tolyl})(\text{PPh}_3)_3$ (150 mg, 0.145 mmol) and B_2cat_2 (47 mg, 0.20 mmol) was dissolved in benzene (15 mL) and the orange solution irradiated for 5 min by a 1000 W tungsten-halogen lamp held 10 cm from the flask. The solution was then stirred at 20 °C for 1.5 h without irradiation. The solvent was removed from the resulting pale yellow solution in vacuo, and CH_2Cl_2 (10 mL) was added. Addition of EtOH (10 mL) and removal of the CH_2Cl_2 in vacuo gave pure **11** as a white microcrystalline solid, which was collected on a glass frit and washed with EtOH and hexane (yield 68 mg, 47%). ^1H NMR spectroscopy showed 0.25 equiv of CH_2Cl_2 present as solvate. Anal. Calcd for $\text{C}_{57}\text{H}_{45}\text{B}_2\text{NO}_5\text{P}_2\text{Ru}\cdot 0.25 \text{CH}_2\text{Cl}_2$: C, 66.79; H, 4.45; N, 1.36. Found: C, 66.93; H, 4.34; N, 1.24.

Os(CCl=C(Cl)Cl)(CO) $_2$ (PPh $_3$) $_2$ (12). A colorless solution of *cis*-Os(Bcat)(*o*-tolyl)(CO) $_2$ (PPh $_3$) $_2$ (100 mg, 0.102 mmol) and C_2Cl_4 (0.50 mL, 4.9 mmol) in benzene (12 mL) was stirred for 16 h at 20 °C to give a pale yellow solution. The benzene was removed in vacuo, and the solid residue was dissolved in CH_2Cl_2 (10 mL). Addition of EtOH (5 mL) followed by removal of the CH_2Cl_2 in vacuo gave pure **12** as a white microcrystalline solid, which was collected on a glass frit and washed with EtOH and hexane (yield 68 mg, 71%). Anal. Calcd for $\text{C}_{40}\text{H}_{30}\text{Cl}_4\text{O}_2\text{OsP}_2$: C, 51.29; H, 3.23. Found: C, 51.76; H, 3.29.

***cis*-Os(Bcat)Cl(CO) $_2$ (PPh $_3$) $_2$ (13).** A stream of CO gas was passed through a solution of Os(Bcat)Cl(CO)(PPh $_3$) $_2$ (100 mg, 0.111 mmol) in CH_2Cl_2 (10 mL) for 5 s, turning it colorless. Addition of EtOH (10 mL) and removal of the CH_2Cl_2 in vacuo gave pure **13** as a white microcrystalline solid, which was collected on a glass frit and washed with EtOH and hexane (yield 93 mg, 90%). Anal. Calcd for $\text{C}_{44}\text{H}_{34}\text{BClO}_4\text{OsP}_2$: C, 57.12; H, 3.70. Found: C, 56.82; H, 3.49.

***trans*-Os(Bcat)(Ph)(CO) $_2$ (PPh $_3$) $_2$ (14).** A solution of LiPh in Et_2O (0.82 M, 0.32 mL, 0.27 mmol) was added slowly to a rapidly stirred colorless solution of *cis*-Os(Bcat)Cl(CO) $_2$ (PPh $_3$) $_2$ (205 mg, 0.222 mmol) in benzene (15 mL) at 5 °C, turning the mixture pale yellow and cloudy. The mixture was allowed to warm to 20 °C and then stirred for 30 min. The benzene was then removed in vacuo and the solid residue dissolved in CH_2Cl_2 (10 mL). Addition of EtOH (5 mL) followed by removal of the CH_2Cl_2 in vacuo gave pure **14** as a white microcrystalline solid, which was collected on a glass frit and washed with EtOH and hexane (yield 137 mg, 64%). Anal. Calcd for $\text{C}_{50}\text{H}_{39}\text{BO}_4\text{OsP}_2$: C, 62.12; H, 4.07. Found: C, 61.96; H, 4.14.

***trans*-Os(Bcat)I(CO) $_2$ (PPh $_3$) $_2$ (16). Method 1.** A mixture of *trans*-Os(Bcat)(*o*-tolyl)(CO) $_2$ (PPh $_3$) $_2$ (107 mg, 0.109 mmol) and I_2 (34 mg, 0.13 mmol) was dissolved in CH_2Cl_2 (15 mL) to give a purple solution, which was stirred for 3 h. Addition of EtOH to the resulting orange solution followed by removal of the CH_2Cl_2 in vacuo gave a yellow solid, which was collected on a glass frit and washed with EtOH and hexane. This solid was then dissolved in CH_2Cl_2 and passed down a column (silica gel/ CH_2Cl_2 /hexane, 1:1 as eluant). The first fraction to elute was yellow, and removal of the solvent in vacuo followed by recrystallization from CH_2Cl_2 /EtOH afforded pure *trans*-Os(*o*-tolyl)I(CO) $_2$ (PPh $_3$) $_2$ (yield 45 mg, 42%). IR (KBr, Nujol): $\nu(\text{CO}) = 1947$ vs cm^{-1} . Anal. Calcd for $\text{C}_{45}\text{H}_{37}\text{IO}_2\text{OsP}_2$: C, 54.66; H, 3.77. Found: C, 54.57; H, 3.86.

The second fraction was colorless, and collection and removal of solvent in vacuo, followed by recrystallization from CH_2Cl_2 /EtOH, afforded pure *trans*-Os(Bcat)I(CO) $_2$ (PPh $_3$) $_2$ as colorless crystals (yield 54 mg, 49%). ^1H NMR spectroscopy showed 0.8 equiv of CH_2Cl_2 present as solvate. Anal. Calcd for $\text{C}_{44}\text{H}_{34}\text{BIO}_4\text{OsP}_2\cdot 0.8 \text{CH}_2\text{Cl}_2$: C, 49.63; H, 3.31. Found: C, 49.66; H, 3.18.

Method 2. A solution of *cis*-Os(Bcat)I(CO) $_2$ (PPh $_3$) $_2$ (141 mg, 0.14 mmol) in toluene (20 mL) was heated under reflux for 1 h. The solution was cooled to 20 °C and concentrated to ca. 1 mL in vacuo. Addition of hexane gave pure **16** as a white microcrystalline solid, which was collected on a glass frit and washed with EtOH and hexane (yield 102 mg, 72%). Characterization was by comparison of spectral properties with those of a sample prepared as above.

***cis*-Os(Bcat)I(CO) $_2$ (PPh $_3$) $_2$ (18).** A solution of NaI (0.460 mg, 3.07 mmol) in EtOH (5 mL) was added to a solution of Os(Ph)Cl(CO)(PPh $_3$) $_2$ (263 mg, 0.307 mmol) in CH_2Cl_2 (15 mL), and the resulting mixture was stirred for 30 min to give a deep red cloudy solution. The solvent was removed in vacuo and the residue extracted into CH_2Cl_2 and filtered through Celite. The solvent was removed from the filtrate in vacuo, and a solution of HBcat (0.035 mL, 0.33 mmol) in benzene (15 mL) was then added. The dark red mixture was heated under reflux for 20 min to give an orange solution, which was cooled to 20 °C. A stream of CO gas was then passed through the solution for 20 s, turning it yellow. The benzene was removed in vacuo and the solid residue dissolved in CH_2Cl_2 (10 mL). Addition of EtOH (10 mL) followed by removal of the CH_2Cl_2 in vacuo gave pure **18** as a white microcrystalline solid, which was collected on a glass frit and washed with EtOH and hexane (yield 213 mg, 68%). Anal. Calcd for $\text{C}_{44}\text{H}_{34}\text{BIO}_4\text{OsP}_2$: C, 51.98; H, 3.37. Found: C, 51.89; H, 3.40.

X-ray Diffraction Studies of 5, 8, 10, 11, 12, 16, and 18. Intensity data were collected using a Bruker SMART diffractometer. Data collection covered either a sphere or hemisphere, and unit cell parameters were from all data with $I > 10\sigma(I)$.

Data were corrected for Lorentz and polarization effects and empirical absorption corrections (SADABS) applied.

Structure solution was by Patterson and difference Fourier methods, and refinement was by full-matrix least-squares of F^2 . All non-hydrogen atoms were allowed to refine anisotropically. Hydrogen atoms were placed geometrically and refined with a riding model with thermal parameters fixed at 20% (50% for methyl groups) greater than the carrier atom. Data collection and refinement parameters are summarized in Table 5.

Programs used for structure solution were SHELXS-97 (G. M. Sheldrick, University of Göttingen, 1997) and SHELXL-97 (G. M. Sheldrick, University of Göttingen, 1997).

Acknowledgment. We thank the Marsden Fund, administered by the Royal Society of New Zealand, for supporting this work and for granting a Postdoctoral Fellowship award to A.W.

Supporting Information Available: Tables of crystal data, collection and refinement parameters, positional and anisotropic displacement parameters, and bond distances and angles for **5**, **8**, **10**, **11**, **12**, **16**, and **18**. This material is available free of charge via the Internet at <http://pubs.acs.org>.

OM0004601